Journal of Physics: Conference Series **3131** (2025) 012044 doi:10.1088/1742-6596/3131/1/012044

An initial study on the environmental value of wind farm control

Samuel Kainz[1], Annamaria Scherzl[1], Adrien Guilloré[1], Abhinav Anand[1] and Carlo L. Bottasso [1]

[1]Wind Energy Institute, Technische Universität München, Boltzmannstr. 15, 85748 Garching bei München, Germany

E-mail: samuel.kainz@tum.de

Abstract. The integration of wind energy into the electrical grid significantly reduces greenhouse gas emissions by displacing conventional power plants. This study presents a novel data-driven approach to quantify the environmental value of wind energy generation through the Marginal Displacement Factor (MDF), expressed in kgCO_2-equivalent per MWh. The MDF captures changes in emissions resulting from incremental variations in wind energy generation within an energy system, while accounting for the time-dependent fluctuations in grid emissions driven by the generation mix and demand-supply dynamics. Using the German energy system and the offshore wind farm Wikinger as a case study, results reveal substantial variability in the MDF and highlight the positive impact of wind energy on grid emission reduction. Furthermore, findings demonstrate that wake steering-based wind farm control for maximum power production can improve the environmental value of a wind farm within the same range as the increase in energy production.

1 Introduction

The energy transition is crucial for mitigating climate change, with renewable energy sources playing a central role in decarbonizing the electricity grid. Wind energy, in particular, is a key driver of this shift due to its significantly lower carbon footprint compared to conventional generation technologies [1, 2]. As the energy mix becomes more diverse, including both fossil-based and renewable sources along with storage technologies and variable demand, grid emissions fluctuate over time. These fluctuations are directly influenced by the generation mix, which is shaped by factors such as power generation, imports and exports, and market imbalances. Consequently, grid emissions are not constant but vary based on supply-demand dynamics, market conditions, and power flows within the grid.

In the dynamic and interconnected energy systems of today, clean generation technologies often displace other – primarily fossil fuel-based – power plants, depending on the operational state of the system. The changes in grid greenhouse gas emissions resulting from an incremental increase in energy produced by a displacing technology is referred to as the Marginal Displacement Factor (MDF), expressed in kilograms of carbon dioxide equivalent per megawatt-hour produced (kgCO_2e/MWh). Similarly, the additional grid emissions generated per incremental increase in demand is termed the Marginal Emission Factor (MEF), measured in the same units as MDF [2]. The determination of MEF and MDF requires the identification of the emissions related to the generators operating at the margin, i.e., those that actively adjust their output to maintain grid balance. To this end, several studies have applied merit order-based approaches, primarily aiming at the estimation of the MEF. Some derived the merit order from historical data [3, 4] or power plant activation criteria [5], while others, such as ref. [6], extended this approach to future energy systems, requiring a detailed modeling of all power plants and their interdependencies.

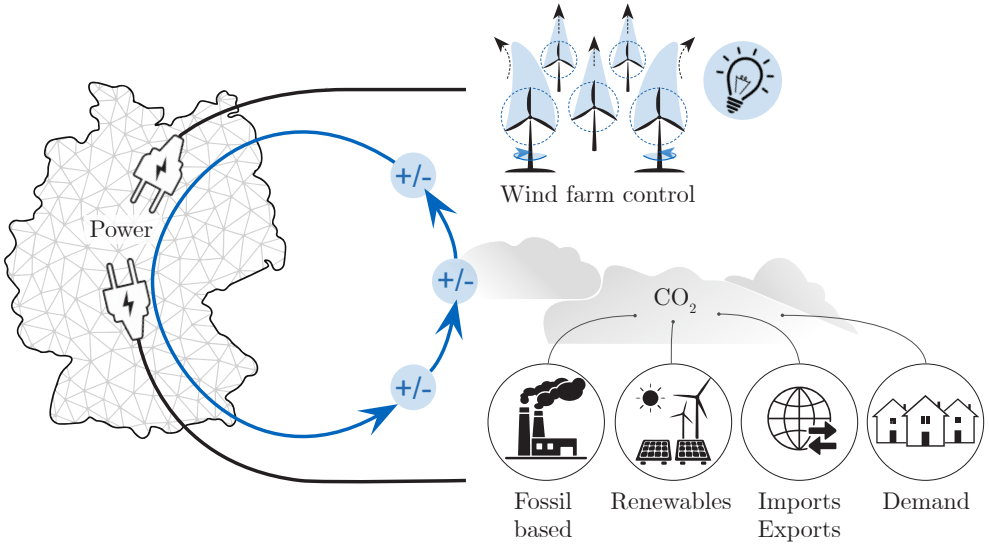

Figure 1: The environmental value of wind farm control: by changing the wind farm power output, wind farm control can marginally alter the generation mix in the connected energy system, ultimately affecting the total grid emissions.

Identifying the marginal generators is a highly complex and market-dependent problem, which is influenced by regulations, policies, dispatch schedules, cross-border transfers, and real-time grid conditions. A data-driven approach offers an effective and straightforward solution, as it implicitly accounts for all the relevant driving factors from both markets and the grid. By capturing these dynamics in a statistical sense, a data-driven model can predict the most likely MEF and MDFs, based on the operational state of the considered energy system. Therefore, previous research has predominantly relied on data-driven approaches, often employing linear regression models. An early study [7] used simple regression analysis to map system emissions to a single system state variable. Later works [2, 8] refined this approach by incorporating additional system variables and accounting for physical limitations of power plants. Ref. [9] further extended the linear regression approach to account for electricity imports and exports. A more recent study [10] applied machine learning to improve the temporal resolution of MEF estimation, but was constrained to a limited set of system state variables in a highly renewable energy system and focused solely on the MEF. In summary, previous research has either relied on identifying the marginal generators within market-specific merit orders – which requires data that is not publicly available and involves large physical models with numerous assumptions – or has been limited to a narrow set of system state variables, to specific case studies, and with a primary focus on the MEF.

To address these limitations, this work introduces a data-driven approach with a general formulation to calculate both the MEF and the MDFs for all considered generation technologies, using standard system data often made publicly available by transmission system operators. The study focuses on the MDF of wind energy and the effects of wind farm control (WFC) on grid emission in particular. Advancements in WFC technologies have significantly improved the ability of wind power plants to generate and deliver additional electricity to the grid, depending on the wind resource availability. This capability enables the estimation of the additional displaced grid emissions attributable to WFC, thereby allowing for a more explicit quantification of the environmental value of WFC, as visualized in Fig. 1. Once quantified, the time-varying nature of the environmental value of WFC could be leveraged to maximize its impact by increasing the power output of the wind farm during time periods when the grid is predominantly supplied by higher-emission power plants. Furthermore, the environmental value of WFC could be assessed alongside its economic value, considering fluctuating energy market conditions and effects of WFC on the structural health of wind turbine components, to develop a multi-objective control strategy that balances economic and environmental sustainability. It is also possible that, in the future, the displacement of carbon-emitting plants might be incentivized, thereby providing an additional revenue stream. While this paper does not directly explore these aspects, the developed method and results provide a foundation for future research on value-based WFC strategy optimization.

2 Methodology

2.1 Time series of emissions

First, the total emissions occurring in the considered energy system are determined from time series. In this study, the scope of an energy system is defined to correspond to the boundaries of a country. However, the approach is more general and can be applied to regions with lower or higher granularity, such as control areas or bilateral market zones.

Since electricity grids are characterised by a high level of interconnectivity, the total emissions E for different operational states of an energy system at a given time t depend on the emissions due to electricity generation within the country as well as the emissions from electricity imports and exports:

$$E(t) = \sum_{k=1}^{N_{tech}} e_k P_k^{gen}(t) + \sum_{nc=1}^{N_{nc}} e_{nc}(t) P_{nc}^{imp}(t) - e_{int}(t) \sum_{nc=1}^{N_{nc}} P_{nc}^{exp}(t). \tag{1}$$

Here, N_{tech} denotes the number of generation technologies operating within the country, P_k^{gen} the aggregated power production from a particular generation technology k, e_k the technology-specific emission intensity, P_{nc}^{imp} the electricity imported from N_{nc} neighbouring countries, e_{nc} the average emission intensity of the respective neighbouring country, P_{nc}^{exp} the electricity exported to a given neighbouring country nc, and e_{int} the average emission intensity due to production within the country under consideration.

The average emission intensity of a neighbouring country e_{nc} at a given time instant t is calculated as

$$e_{nc}(t) = \frac{\sum_{k=1}^{N_{tech}^{nc}} e_k P_k^{gen}(t)}{\sum_{k=1}^{N_{tech}^{nc}} P_k^{gen}(t)}, \tag{2}$$

where N_{tech}^{nc} denotes the number of generation technology in the neighbouring country nc.

Similarly, the average emission intensity due to production within the country under consideration e_{int} is calculated as

$$e_{int}(t) = \frac{\sum_{k=1}^{N_{tech}} e_k P_k^{gen}(t)}{\sum_{k=1}^{N_{tech}} P_k^{gen}(t)}. \tag{3}$$

To simplify the notation, the dependency on time t is omitted in the following.

2.2 Marginal displacement vector

As shown in the previous section, the time-varying overall system emissions depend on the generation mix of the considered country as well as the imports and exports from the neighbouring countries. The electricity supply, in turn, depends on the electricity demand within the country. Therefore, the total system emissions E can be expressed as

$$E = f(\underline{p}), \tag{4}$$

where $\underline{p}$ is a column vector of length p containing the system state variables demand D, all various generation technologies within the grid such as wind energy P_w, photovoltaic P_s, gas, coal, nuclear, etc., and imports P_{imp} and exports P_{exp} to and from neighbouring countries:

$$\underline{p} = [D, P_w, P_s, ..., P_{imp}, P_{exp}]^\top. \tag{5}$$

Next, Principal Component Analysis (PCA) is used to reduce the dimensionality of the problem and decouple the features by transforming them into a set of uncorrelated principal components, minimizing interdependencies while retaining the most significant variance in the data. This can be written as

$$\underline{p} - \underline{p}_m = \mathbf{T}\underline{\Theta}, \tag{6}$$

where $\underline{p}_m$ is the mean of $\underline{p}$, ensuring data centering for PCA, $\underline{\Theta}$ is the vector of length θ containing the principal components, and $\mathbf{T}$ is a transformation of coordinates with dimension $p \times \theta$, which is numerically calculated using the Matlab implementation of PCA [11]. An Artificial Neural Network (ANN) Y, described in detail in the next section, is used to map the principal components to the total system emissions. Therefore, Eq. (4) can be rewritten as:

$$E = Y(\underline{\Theta}). \tag{7}$$

The changes in system emissions with respect to infinitesimal changes in the system state variables can be determined via the partial derivative of Eq. (7), resulting in the definition of the marginal displacement $\delta e = -\delta E$, which writes

$$\delta e = -\left(\frac{\partial \mathrm{Y}}{\partial \underline{\Theta}}\right)^{\top} \delta \underline{\Theta}. \tag{8}$$

The negative sign ensures that marginal displacements are positive when emissions are displaced and negative when additional emissions are generated in the considered energy system.

Next, the grid balance constraint is introduced, ensuring that changes in demand are always met by supply and vice versa:

$$\underline{v}^{\top} \delta \underline{p} = \underline{n}^{\top} \delta \underline{p} = 0, \tag{9}$$

with $\underline{v}$ being a column vector of length p containing a value of -1 at the position occupied by demand in vector $\underline{p}$ and 1s elsewhere, and $\underline{n}$ being the unit vector of $\underline{v}$:

$$\underline{v} = [-1, 1, 1, ..., 1]^{\top}, \quad \underline{n} = \frac{1}{\sqrt{p}} \underline{v}, \quad \underline{n}^{\top} \underline{n} = \underline{1}. \tag{10-12}$$

Given an arbitrary variation $\delta \underline{p}$, the corresponding variation that satisfies the grid balance constraint writes

$$\delta \underline{p}^{*} = \left(\mathbf{I} - \underline{n}\underline{n}^{\top}\right) \delta \underline{p}. \tag{13}$$

Combining Eq. (6), (8) and (13) leads to the definition of the marginal displacement vector:

$$\frac{\partial e}{\partial \underline{p}} = -\left(\frac{\partial \mathrm{Y}}{\partial \underline{\Theta}}\right)^{\top} \mathbf{T}^{\top} \left(\mathbf{I} - \underline{n}\underline{n}^{\top}\right). \tag{14}$$

This marginal displacement vector contains the MEF at the location of D in vector $\underline{p}$, and the MDFs for the respective generating technologies as well as imports and exports at their respective positions in $\underline{p}$.

The derivatives of the emission function with respect to the principal components, noted

$$\frac{\partial \mathrm{Y}}{\partial \underline{\Theta}} = \left[\frac{\partial \mathrm{Y}}{\partial \Theta_1}, \frac{\partial \mathrm{Y}}{\partial \Theta_2}, ..., \frac{\partial \mathrm{Y}}{\partial \Theta_{\Theta}}\right]^{\top}, \tag{15}$$

are calculated numerically using central finite differences applied to the trained ANN:

$$\frac{\partial \mathrm{Y}}{\partial \Theta_i} = \frac{Y(\Theta_i + \Delta\Theta_i) - Y(\Theta_i - \Delta\Theta_i)}{2\Delta\Theta_i}. \tag{16}$$

Notice that the principal components are orthogonal to each other and therefore represent independent features. The step size $\Delta\Theta_i$ is determined by multiplying the relative step width w with the quantile span between the 2.5% quantile $Q_{2.5}$ and the 97.5% quantile $Q_{97.5}$ of the respective principal components:

$$\Delta\Theta_i = w\left(Q_{\Theta_i,97.5} - Q_{\Theta_i,2.5}\right). \tag{17}$$

2.3 Artificial neural network for emission prediction

An ANN is trained to predict the grid emissions for a given set of system state variables at a specific time. The ANN is implemented in Matlab [12] as a shallow feed-forward network with one hidden layer containing 350 neurons. The network is trained for 500 epochs using the Levenberg-Marquardt optimization algorithm based on default values [12], with hyperbolic tangent activation functions in both the hidden layers and the output layer. The dataset is split into 65% for training, 20% for validation, and 15% for testing. The model performance is evaluated using the R^2 score, where a value of 1 indicates perfect correlation between predicted and actual values, and the Root Mean Squared Error (RMSE), which quantifies the average prediction error in the same units as the target variable. The inputs and target datasets are normalized to a range between 0 and 1 to improve training stability and performance.

The number of neurons and epochs are selected such that the ANN predictions are robust not only for the target function but also for its derivatives, as required for the calculation of the MDF according to Eq. (14). Figure 2 presents the results of a parametric study exploring different neuron and epoch configurations using the dataset described in the *Results* section. The network performance, along with the mean and standard deviation (SD) of both total system emissions and the MDF of wind, are used

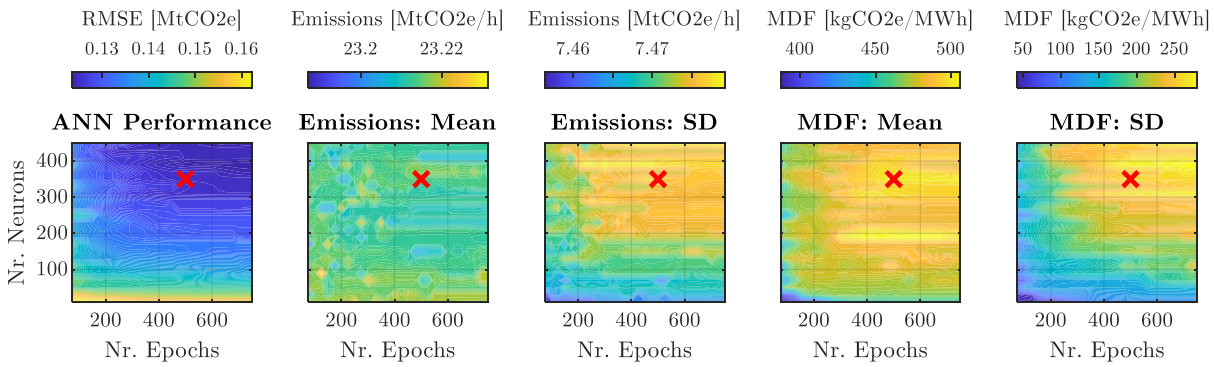

Figure 2: Results of the parametric study investigating the effects of varying number of neurons and epochs on the ANN performance (RMSE of the system emissions), ANN target prediction in terms of mean and standard deviation of the system emissions, and prediction of the MDF of wind in terms of mean and standard deviation. The red cross marks the selected configuration for the case study.

as performance indicators. The final configuration is manually chosen as a trade-off between robustness, computational efficiency, and minimizing the risk of overfitting. As the MDF exhibits significant sensitivity to the selected training function, the impact of the training function choice, along with the propagation of uncertainties in data and model parameters, will be investigated in a follow-up study.

The target grid emissions are calculated according to Eq. (1). Table 1 lists the final set of input variables for the ANN. To simplify the input features, imports and exports are aggregated as total net imports and total net exports across all neighboring countries. This differs from the approach used to calculate the ANN target emissions, where imports and exports are treated separately for each neighboring country, reducing complexity and computational demand while still capturing essential system dynamics. Time series data for electricity generation, imports, and exports are taken from the open-source ENTSO-E Transparency Platform [13]. Electricity demand is computed as the net sum of generation, imports, and exports. Table 1 provides the corresponding ENTSO-E data tags for each input variable. Each dataset is downloaded at the highest available frequency and subsequently resampled to quarter-hourly time steps.

Emission intensities for the considered technologies are sourced from the ecoinvent database v3.7.1 [1], using the 'Allocation cut-off by classification' system model. Germany is selected as the geographic scope, serving as a representative reference for emission intensities across the studied European countries. Emission intensities are adjusted to include only operational emissions of the generating technologies, as only these can be displaced in real-time on the electrical grid. On the other hand, life-cycle emissions linked to infrastructure such as powerplants, transmission or distribution grids are omitted because they cannot be displaced by a change in wind power generation. Transmission and distribution losses are implicitly included in the original datasets.

2.4 Wind farm performance and control optimization

The simulation software FLORIS [14] is used to calculate both the baseline power production and the increased power potential achieved through wake steering. Velocity deficits are calculated using the Jensen model [15] with a wake decay coefficient of 0.05 and are combined via root-sum-square superposition. Wake deflections are determined using the Jiménez model [16] with default parameters. The Serial-Refine method [17] is applied to generate look-up tables with optimized yaw angles ranging from -30° to +30° for each turbine, considering all possible combinations of ambient wind speed and wind direction. Discretization is set to 1 m/s for wind speed, 1° for main inflow directions, and 2.5° for other directions. Optimum yaw angles are then linearly interpolated to accommodate any arbitrary combination of wind speed and direction within the operational regime.

3 Results

3.1 Marginal displacement factor in Germany

As a first step, the proposed method for calculating the MDF of wind is applied to the German energy system, using time series data from 2021 and 2022. After performing PCA, five principal components are retained, capturing more than 97% of the total initial variance. Half of the shuffled dataset is used

ANN Feature	Column(s) in ENTSO-E dataset [13]	ecoinvent base activity [1] (adapted for direct operational emissions only)	Emission Factor ($kgCO_2e/MWh$)
Demand	Domestic supply[1]	-	acc. to Eq. (1)[2]
Wind	Wind Offshore[3]	electricity prod., wind, 1-3MW turbine, offshore	0.2
	Wind Onshore[3]	electricity prod., wind, 1-3MW turbine, onshore	0.2
Solar	Solar[3]	electricity prod., photovoltaic, 570kWp open ground	0.0
Lignite	Fossil Brown coal / Lignite[3]	electricity prod., lignite	1221.9
Hard coal	Fossil Hard coal[3]	electricity prod., hard coal	1049.6
Oil	Fossil Oil[3]	electricity prod., oil	846.5
Gas	Fossil Gas[3]	electricity prod., natural gas, conv. power plant	421.8
Nuclear	Nuclear[3]	electricity prod., nuclear, pressure water reactor	4.4
Hydro	Hydro Pumped Storage[3]	electricity prod., hydro, pumped storage	883.1
	Hydro Run-of-river[3]	electricity prod., hydro, run-of-river	0.0
	Hydro Water Reservoir[3]	electricity prod., hydro, reservoir, non-alpine region	44.8
Other RE	Geothermal[3]	electricity prod., deep geothermal	0.0
	Marine[3]	average of used renewable emission factors	122.6
	Other renewable[3]	average of used renewable emission factors	122.6
	Biomass[3]	heat and power co-generation, wood chips, 6667 kW	52.6
	Waste[3]	zero since emissions are allocated to waste producer	0.0
Other Conv.	Other[3]	average of used conventional emission factors	885.0
	Fossil Coal-derived gas[3]	average of used conventional emission factors	885.0
	Fossil Oil shale[3]	average of used conventional emission factors	885.0
	Fossil Peat[3]	average of used conventional emission factors	885.0
Imports	Neighbors to Germany[4]	-	acc. to Eq. (2)
Exports	Germany to neighbors[4]	-	acc. to Eq. (3)

[1] Electricity demand is computed as the net sum of inland generation, imports, and exports.
[2] The total emissions E derived from Eq. (1) are divided by the electricity demand.
[3] ENTSO-E dataset: Actual Generation per Production Type
[4] ENTSO-E dataset: Cross-Border Physical Flow

Table 1: Features of the artificial neural network, used ENTSO-E datasets with associated specifications [13], as well as emission factors and their corresponding base activities from the ecoinvent database [1].

for training the ANN, achieving R^2 scores of 0.996 for training and 0.995 for testing. The full time series is used for the statistical analysis of the MDF, while two representative weeks – one in winter and one in summer – are selected for demonstration purposes. However, given the nature of the underlying open-source database [13], this analysis can easily be extended to any country, market, or control zone within the European Union using data from the past ten years.

The step width w required for Eq. (17) is determined first. Figure 3 illustrates the effect of varying the step width on the mean and SD of the MDF of wind. As expected, these metrics converge for sufficiently small step widths. Within this study, the proposed method is intended to analyze the environmental value of both the baseline production and the effects of WFC in a 350 MW wind farm, as described in the next section. Therefore, the step width is determined by perturbing the wind energy production in the studied time series by the rated power of the wind farm, calculating the resulting changes in the principal components, and comparing them with the step size defined in Eq. (17). This process yields a maximum allowed step width of 1.51%, which, as shown in Fig. 3, is considered to be sufficiently small.

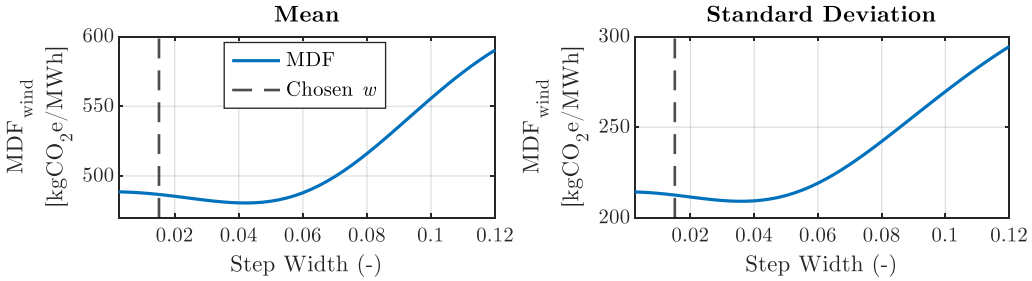

Figure 3: Impact of the step width w on the mean and standard deviation of the MDF of wind. A dashed line indicates the step width selected for the case study.

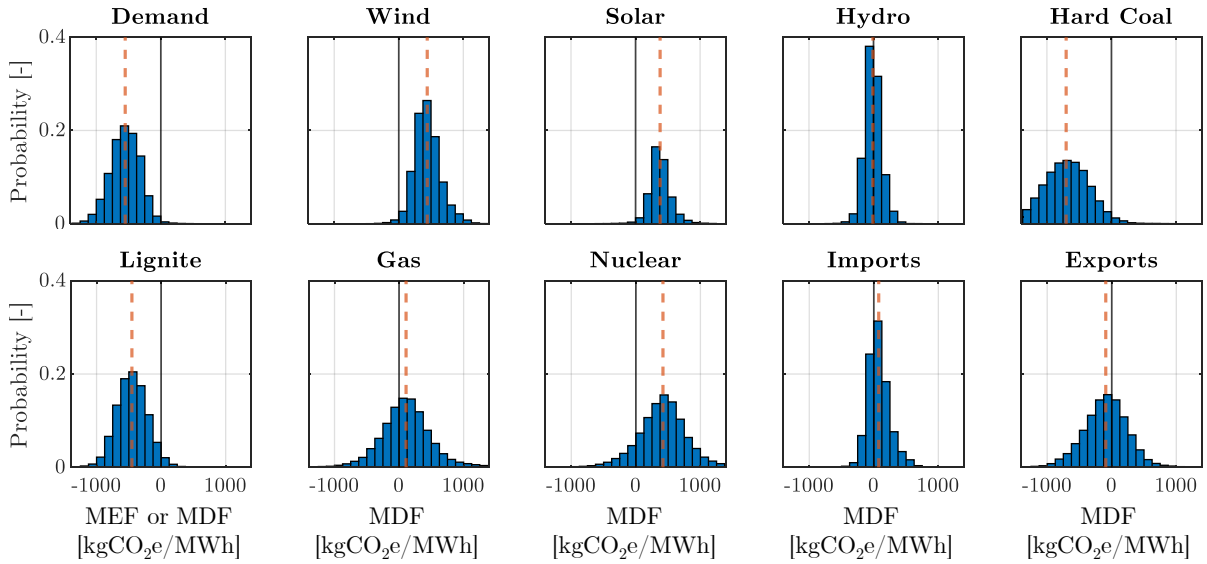

Figure 4: Histogram distributions of MEF and MDFs for the 10 main considered features in Germany during 2021 and 2022. The mean values are indicated by orange dashed lines.

While this analysis primarily focuses on the MDF of wind energy, the proposed method is capable of predicting the MEF and the MDF for all features involved. Accordingly, Fig. 4 presents the histograms and mean values for the MEF and MDF distributions of the 10 most significant features. Wind, solar, and nuclear power generally exhibit positive MDFs, indicating a beneficial impact on the grid emissions. In contrast, increased demand, as well as increased hard coal and lignite generation, typically worsen the environmental performance of the grid. Hydropower, gas, imports, and exports have either positive or negative environmental impacts, depending on the other system state variables. The widespread variation in the MDF distributions underscores the importance of accounting for their time-dependent nature when assessing the environmental value of these technologies at a specific moment. The MDF of wind has an average value of 441.1 $kgCO_2e/MWh$, with a 99% data-based confidence interval ranging from -88.6 to 1,068.7 $kgCO_2e/MWh$. This indicates that wind energy is displacing various combinations of generators across most of the studied generational technologies as listed in Table 1, with an average impact comparable with the emission factor of gas power plants. However, wind energy can sometimes cause additional emissions in the grid when the MDF of wind is negative, which may be either associated with phenomena like congestion management requiring fossil power plants for compensation or numerical errors in the ANN, warranting further research. The fact that the other MDF distributions also fall within the physically plausible ranges of the studied generation technologies – except for a few outliers due to numerical errors – supports the validity of the proposed method for calculating MDFs.

As expected, wind energy generation primarily causes a positive impact on the environmental performance of the grid, although the magnitude of this effect is highly time-dependent. To explore this further, Fig. 5 presents two sample time series from Germany in 2022, illustrating the generation mix, imports and exports, total system emissions, and MDF of wind during two exemplary weeks in summer and winter, respectively. The winter week is characterised by strong wind but limited solar availability, significant gas-fired generation, and substantial electricity exports. In contrast, the summer week exhibits a slightly lower demand, less wind but abundant solar resources, and fluctuating shifts between net imports and exports due to solar variability. In both cases, the total system emissions highly depend on the availability of wind and solar resources. Notably, the system emissions predicted by the ANN align well with those calculated using Eq. (1), reinforcing the previously reported high R^2 performance indices.

The MDF of wind exhibits significant variability, ranging from -53.9 to 1,215.1 $kgCO_2e/MWh$ in the exemplary winter week, with a weekly average of 555.1 $kgCO_2e/MWh$. In the summer week, values range from -237.1 to 1089.4 $kgCO_2e/MWh$, with an average of 426.4 $kgCO_2e/MWh$. These findings align with the previously presented statistical analysis of the full two-year time series, but suggest that MDF values tend to be higher in winter. Additionally, the MDF of wind shows distinct daily fluctuations, often reaching its lowest values around noon and peaking around midnight. Pronounced shifts seem to occur during periods of rapid changes in solar and wind energy generation.

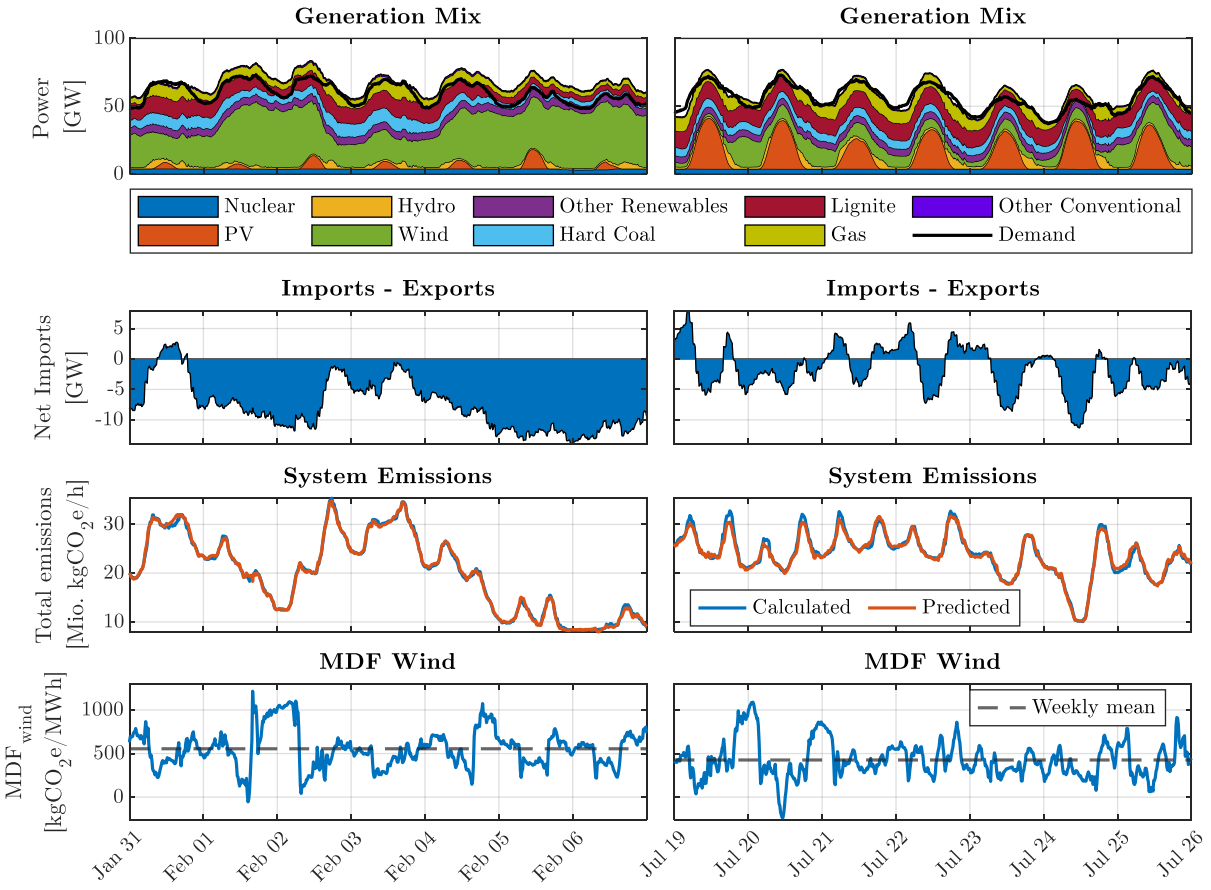

Figure 5: Time series of supply, demand, calculated and predicted system emissions, and the MDF of wind for two exemplary weeks in winter (left) and summer (right) in Germany in 2022.

3.2 Displaced emissions through wind farm control

The environmental value of both the baseline performance of a wind farm and the effects of WFC is evaluated using the offshore wind farm Wikinger [18] for the year 2022 as a case study. Wikinger was commissioned in 2017, is located in the Baltic Sea, and is connected to the German electricity grid. The wind farm consists of 70 turbines with a total nominal capacity of 350 MW, and is modeled in FLORIS, as described in Sect. 2.4. Due to limited access to the actual turbine performance curves, the Adwen AD5-135 turbines are replaced with NREL 5-MW Reference Turbines [19], which have the same rated power and a similar rotor diameter. The hub height is set to its actual value of 97.5 m. Hourly inflow time series are obtained from ERA5 [20], with wind speed scaled to hub height using the power law with the alpha exponent determined for each time step based on the reference wind speeds at a height of 10 m and 100 m, respectively. The turbine positions are extracted from OpenStreetMap data [21].

As shown in Fig. 6, the farm layout is well-suited for enhancing total power output through yaw-optimized wake steering. Over the course of 2022, the calculated baseline energy production of 1400.8 GWh can be increased by 3.15% through WFC using wake steering. The associated grid emissions displaced by Wikinger are determined by multiplying the time series of the wind farm power production with the corresponding values for MDF of wind. Accordingly, Wikinger displaced 686.6 $MtCO_2e$ in 2022, with a potential increase of 2.99% through wake steering. On average, the electricity displaced by Wikinger corresponds to emissions of 490.3 $kgCO_2e/MWh$. This value is 25 to 77 times higher than the carbon footprint of typical offshore wind farms [22], underscoring the significant role of wind energy in reducing the carbon intensity of the connected energy system.

Finally, Fig. 7 illustrates the wind farm power production and the corresponding displaced grid emissions, both with and without wake steering, for the same two exemplary weeks analyzed previously. The respective weekly means are indicated by dashed lines. In both weeks, the baseline production of Wikinger fluctuates significantly between zero and nominal capacity due to wind variability, with higher

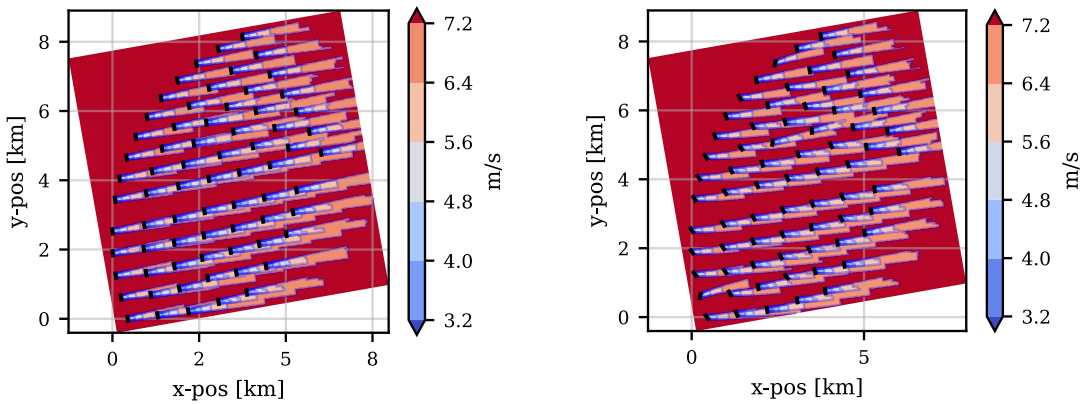

(a) Baseline **(b)** Wake Steering

Figure 6: Flow field at the Wikinger wind farm for the main inflow direction and mean wind speed, shown for **(a)** the baseline scenario, and **(b)** the wake steering scenario, visualized with FLORIS [14].

average power outputs in the winter week due to better resource availability. The trend in displaced grid emissions generally follows the power production but exhibits notable deviations due to the pronounced variability of the MDF of wind, as discussed earlier. This effect is particularly evident during periods of rated power production, where the power output remains constant while the displaced grid emissions fluctuate considerably. Similarly, the trends in additional power production and increased displaced emissions due to wake steering follow similar patterns, while relative changes sometimes differ significantly. Gains of up to 38.3 MW for power and 14.8 tCO_2e/h for emissions displacements are observed, with their peaks occurring at different times. On average, wake steering yields higher benefits in the summer week, as the wind farm operates less frequently at rated power, leaving more room for incrementing the power

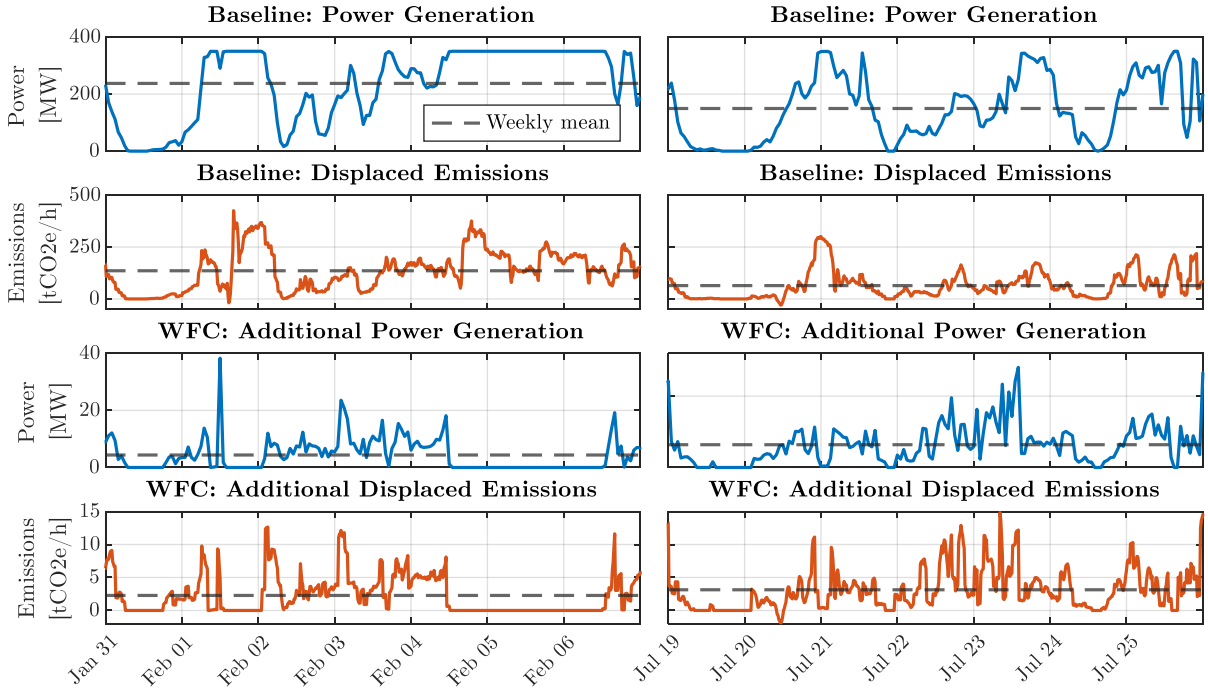

Figure 7: Time series of the baseline power generation and displaced emissions at Wikinger, and additional benefit from wake steering, for two exemplary weeks in winter (left) and summer (right) in 2022.

output when sufficient wind is available. Notably, at two instances, the wind farm production slightly increases the grid emissions due to a negative MDF of wind. This effect could be mitigated through control actions, such as shutting down turbines at such moments. Further investigation into these negative values and their impact on control strategies will be subjects of future research.

4 Conclusion

This paper presented a novel data-driven method for calculating the time-varying grid emission displacements related to demand, generation technologies, and import and exports of a given country, control or market zone, with a particular focus on the MDF of wind energy. The approach was demonstrated for the German energy system in the years 2021 and 2022. The environmental performance of an offshore wind farm connected to the German electricity grid was evaluated both for its baseline operation and for potential improvements through wake steering-based WFC. Overall, wind energy generation significantly reduces grid emissions, with average emission displacements comparable to the emission factor of gas power plants. The case study of the Wikinger offshore wind farm showed that wake steering for maximum power production could enhance the environmental performance of the farm by approximately 3%, which is within the range of the observed increases in energy yield. However, the time-dependent nature of the MDF of wind leads to considerable fluctuations in the environmental performance of wind farms, with displaced emissions spanning the entire portfolio of typical generation technologies. Future work will focus on optimizing operational strategies to maximize the environmental benefits. Additionally, trade-offs involving energy yield, fatigue loads, reliability, and economic revenue will be explored, along with the simultaneous optimization of environmental-aware control strategies and layout of a wind farm.

Acknowledgement

This work has been partially supported by the MERIDIONAL, the SUDOCO, and the TWAIN projects, which receive funding from the European Union's Horizon Europe Programme under the grant agreements No. 101084216, No. 101122256 and No. 101122194, respectively. The authors acknowledge Irène Apra for the design of Fig. 1.

References

[1] Wernet G, Bauer C, Steubing B, Reinhard J, Moreno-Ruiz E and Weidema B 2016 *Int J Life Cycle Assess* **21** 1218–1230
[2] Thomson R C, Harrison G P and Chick J P 2017 *Energy Policy* **101** 201–210
[3] Schram W, Lampropoulos I, AlSkaif T and Van Sark W 2019 *SMARTGREENS 2019 - Proceedings of the 8th International Conference on Smart Cities and Green ICT Systems* (SciTePress) pp 187–193
[4] Marnay C, Fisher D, Murtishaw S, Phadke A, Price L and Sathaye J 2002 Estimating carbon dioxide emissions factors for the california electric power sector Tech. rep. Berkeley Lab
[5] Voorspools K 2000 *Energy* **25** 1119–1138 ISSN 03605442
[6] Böing F and Regett A 2019 *Energies* **12** 2260
[7] Hawkes A D 2010 *Energy Policy* **38** 5977–5987 ISSN 03014215
[8] Jansen M, Staffell I and Green R 2018 *15th Int. Conf. on the EEM* (IEEE) pp 1–5
[9] Oliveira T, Varum C and Botelho A 2019 *Energy Economics* **80** 48–58
[10] Mayes S, Klein N and Sanders K T 2024 *Journal of Cleaner Production* **434**
[11] The MathWorks Inc 2022 Statistics and Machine Learning Toolbox version: 12.4 (R2022b)
[12] The MathWorks Inc 2022 Deep Learning Toolbox version: 14.5 (R2022b)
[13] ENTSO-E Transparency Platform `https://transparency.entsoe.eu/` accessed: 2024-04-28
[14] NREL 2024 FLORIS Version 4.1 `https://github.com/NREL/floris` Accessed 2024-07-04
[15] Jensen N 1983 *A note on wind generator interaction* (*Risø-M* no 2411)
[16] Jiménez Á, Crespo A and Migoya E 2010 *Wind Energy* **13** 559–572
[17] Fleming P A, Stanley A P J, Bay C J, King J, Simley E, Doekemeijer B M and Mudafort R 2022 *Journal of Physics: Conference Series* **2265** 032109
[18] Iberdrola Wikinger wind farm `www.iberdrola.de/unsere-projekte/offshore/wind-wikinger` accessed: 2024-08-28
[19] Jonkman J, Butterfield S, Musial W and Scott G 2009 Definition of a 5-MW Reference Wind Turbine for Offshore System Development Tech. rep. NREL
[20] Munoz Sabater J 2019 ERA5-Land hourly data from 1981 to present Copernicus Climate Change Service (C3S) Climate Data Store (CDS). Accessed: 2024-07-04
[21] OpenStreetMap contributors 2017 Planet dump retrieved from https://planet.osm.org
[22] Kouloumpis V and Azapagic A 2022 *Sustainable Production and Consumption* **29** 495–506